BMC Medical Genomics

RESEARCH

Open Access

Comprehensive analysis of diagnostic biomarkers related to histone acetylation in acute myocardial infarction

Man Li[1,2,3], Lifeng Yang[1,2,3], Yan Wang[1,2,3] and Lei Zhang[1,2,3*]

Abstract

Background Acute myocardial infarction (AMI) has become a serious disease that endangers human health, with high morbidity and mortality. Numerous studies have reported histone acetylation can result in the occurrence of cardiovascular diseases. This article aims to explore the potential biomarkers of histone acetylation regulatory genes (ARGs) in AMI patients.

Methods Five AMI datasets were downloaded from the Gene Expression Omnibus (GEO) database. Next, ARG-related genes were gathered by gene set variation analysis (GSVA) and Spearman's correlation analysis. Subsequently, weighted gene co-expression network analysis (WGCNA) was performed to identify the module genes related to histone acetylation regulation. In the GSE60993 and GSE48060 datasets, the common differentially expressed genes (DEGs) between AMI and control samples were screened. Importantly, the intersecting genes were obtained by overlapping ARGs-related genes, common DEGs, and module genes. Then, the biomarkers in AMI were determined by machine learning, receiver operating characteristic (ROC) curves, and quantitative PCR (qPCR). In addition, immune analysis, drug prediction, molecular docking, and the lncRNA-miRNA-mRNA regulatory network targeting the biomarkers were analyzed, respectively.

Results Here, a total of 18 intersecting genes were identified by overlapping 7,349 ARGs-related genes, 5,565 module genes, and 25 common DEGs. Further, five biomarkers (*AQP9*, *HLA-DQA1*, *MCEMP1*, *NKG7*, and *S100A12*) were obtained, and a nomogram was constructed and verified based on these biomarkers. Notably, the biomarkers were significantly associated with CD8 T cells and neutrophils. In addition, the drugs related to biomarkers were predicted, and ATOGEPANT with the molecular target (*S100A12*) had a high binding affinity (docking score = -10 kcal/mol).

Conclusion *AQP9*, *HLA-DQA1*, *MCEMP1*, *NKG7*, and *S100A12* were identified as biomarkers related to ARGs in AMI, which provides a new perspective to study the relationship between ARGs and AMI.

Keywords Acute myocardial infarction, Histone acetylation, Biomarkers, Machine learning, Quantitative PCR

*Correspondence:
Lei Zhang
lm41669683@126.com
[1]Department of Cardiology, Shanxi Bethune Hospital, Taiyuan, China
[2]Tongji Shanxi Hospital, Taiyuan, China
[3]Third Hospital of Shanxi Medical University, Taiyuan, China

Background

In people's daily lives, cardiovascular disease (CVD) is very common, harmful to human health, and easily causes disability and even death of patients [1]. Acute myocardial infarction (AMI) is a common type, which is caused by coronary artery disease, which poses great harm to human health and even life safety. At present, AMI has become an important cause of disability and even death of patients [2]. In the process of clinical treatment for this disease, taking into account the characteristics of the disease, the focus of treatment is to timely and effective revascularization of the patient's coronary artery to promote the recovery of blood flow. However, early diagnosis is the foundation for timely revascularization. The bioinformatics method has attracted much attention, but it is not applied enough in the research of atherosclerosis cardiovascular disease prevention. It is expected to become an important tool for doctors to promote the precise medical treatment and personalized treatment of atherosclerosis cardiovascular disease [3]. The role of epigenetic regulatory genes in atherosclerosis has been widely studied and considered as important biomarkers and potential therapeutic targets in disease monitoring [4]. Transcription factors and epigenetic mechanisms play a key role in the pathophysiological process of atherosclerosis, involving the influence of epigenetic modifications on transcription factor binding, expression and chromatin remodeling [5]. Research has shown that low methylation of the specific region of the HLA-G gene 5'UTR CpG island is more significant in non critical stenosis coronary heart disease (CHD) patients than in individuals with coronary artery stenosis [6]. In addition, the methylation changes of AIRE1 and ALOX12 promoters can be used as a new epigenetic marker of atherosclerosis [7].

Histone acetylation means that histone acetyltransferase catalyses the acetyl group of Acetoacetyl coenzyme A to bind to the corresponding target of histone, so as to relax the ribosome and activate transcription [8]. A study of myocardial injury has found that histone acetylation regulation-related genes undergo significant changes under the stimulation of cardiac injury, and the activated HDAC4 (histone acetylation regulation gene) induces myocardial injury reperfusion [9]. Histone acetylation plays a significant role in various ischemia-reperfusion-induced tissue injuries. Previous studies have also confirmed that reversible protein acetylation participates in pathological heart remodelling and plays a significant role in the Ischemia/Reperfusion (I/R) environment [10]. In the past, some scholars have reported through research that there is a certain correlation between the occurrence of ischemic heart disease and acetylation induced by histone deacetylase [11]. Recently, some new evidence shows that histone acetylation will participate in the process of oxidized low-density lipoprotein (oxLDL)-induced atherosclerosis. Meanwhile, oxLDL can also affect the expression of some factors in endothelial cells through histone acetylation [12, 13]. And meanwhile, some scholars have also pointed out through research that oxLDL has a positive effect in reducing the level of inflammatory response. Meanwhile, the study also pointed out that Aspergillus A, as a histone deacetylase inhibitor, can have a salvage effect on this inhibitory effect [14]. It can be seen that histone acetylation plays an important role in the inflammatory process of atherosclerosis, and there is a very close correlation with the occurrence of inflammation. Therefore, oxLDL can affect histone acetylation, leading to the change of its expression level. In addition, combined with the research results of some scholars, it was found that the upregulation of H3K9 and H3K27 acetylation levels in activated smooth muscle cells plays an important role in effectively stabilizing plaques [15]. SMC apoptosis will cause plaque rupture, significantly increase the incidence rate, and increase the risk of death of patients. At the same time, the activation of metalloproteinases will also have the above effects [16]. Some scholars have found that histone acetylation can have a certain impact on some factors related to atherosclerosis.

In addition, there are also reports that the rise of MMP-3 level will cause plaque rupture [17]. In the past, some scholars have conducted relevant research from the perspective of epigenetics and pointed out that there is a certain connection between histone acetylation and MMP expression [18]. Therefore, in this stage, histone acetylation will affect the expression of MMP, and make atherosclerosis have certain invasiveness through the rise of this indicator level. In clinical practice, in order to effectively improve the management level of AMI patients and maximize their survival rate, it is necessary to make rapid and accurate diagnoses of the disease. At present, there is some strong evidence that troponin can be used as an important biomarker for detection and analysis in the clinical diagnosis of this disease. Meanwhile, previous studies have also confirmed that cTn levels are elevated in patients with some types of cardiovascular disease other than AMI [19]. However, in order to improve the analysis and diagnostic effectiveness of diseases, we still need to actively analyse, explore, and screen more new and reliable biomarkers, improve the accuracy and sensitivity of clinical diagnosis, and better improve the clinical diagnosis and analysis management effectiveness of diseases. The use of bioinformatics can identify the cardiovascular disease modules behind disturbances in interaction groups, which provides insights into the mechanisms of cardiovascular disease. Biomarkers and drug targets provide new insights [20]. Protein protein interaction (PPI) represents the direct and specific physical binding of two

proteins, providing a more comprehensive understanding of biologically relevant interactions [21]. Therefore, this study is based on bioinformatics and uses machine learning and the protein-protein interaction (PPI) networks to screen a new set of biomarkers. At the same time, it analyses the biological pathways, immune characteristics, and potential drugs that biomarkers may participate in, providing new insights of histone acetylation that may participate in AMI.

Methods

Data source

From the Gene Expression Omnibus (GEO) database (https://www.ncbi.nlm.nih.gov/gds), five AMI dataset s (GSE60993, GSE48060, GSE61144, GSE24548, and GSE97320) were downloaded, respectively. A total of 17 blood samples from AMI patient (patients with acute coronary syndromes undergoing primary percutaneous coronary intervention within 4 h of the onset of chest pain), and seven control blood samples (normal coronary angiograms) from GSE60993 were included. A total of 31 blood samples from patients with first acute myocardial infarction collected within 48 h, and 21 control blood samples (echocardiogram normal) from GSE48060 were included. A total of 7 blood samples from AMI patient (patients with acute coronary syndromes undergoing primary percutaneous coronary intervention within 4 h of the onset of chest pain), and 10 control blood samples (healthy subjects with normal coronary angiograms) from GSE61144 were used as the validation set. The miRNA expression profiling dataset GSE24548 contained four platelet samples from AMI patient (platelets in patients with acute myocardial infarction within 6 h of symptom onset) and 3 control samples (no cardiovascular disease). The lncRNA expression profiling dataset GSE97320 contained 3 blood samples from AMI patient and 3 control samples. A total of 77 histone acetylation regulatory genes (ARGs) were downloaded from previous studies [22], including 22 writers, 18 erasers, and 43 readers, among which six genes serve as both writers and readers (Supplementary Table 1). The flow chart of this study is shown in Supplementary Fig. 1.

Identification of ARGs-related genes

The gene set variation analysis (GSVA) of ARGs in AMI and control samples in the GSE60993 dataset was performed using the GSVA package (version 1.48.3) [23]. Correlations between genes in the GSE60993 dataset and scores of ARGs were calculated to obtain ARGs-related genes ($|cor| > 0.4$, $P < 0.05$). The most relevant modules with scores of ARGs were screened by Weighted Gene Co-Expression Network Analysis (WGCNA) in GSE60993 using the WGCNA package (version 1.73) [24]. First, the samples were clustered to remove outliers. And then, the determination of the soft threshold (β) was performed ($R^2 = 0.8$). The co-expression matrix was established, identifying gene modules and labelling them with different colours (minimum 30 genes per module). The modules with the highest relevance to scores of ARGs were defined as key modules, and intersecting ARGs-related genes were obtained by overlapping the key module and ARGs-related genes.

Differential expression analysis and acquisition of intersecting genes

Differential expression analysis was performed using the limma package (version 3.52.2) in AMI and control samples in the GSE60993 and GSE48060 datasets, respectively, and the ggplot2 package (version 3.3.6) was used to display heatmaps and volcano plots of the expression of the differential genes. The thresholds were set to $|log2FC| > 0.5$ and $P < 0.05$ [25]. Differentially expressed genes (DEGs) obtained in the GSE60993 were defined as DEGs1. DEGs obtained in the GSE48060 were defined as DEGs2. Intersecting DEGs were obtained by taking the intersection of DEGs1 and DEGs2 (up- and down-regulated genes intersection were taken separately). Intersecting genes were obtained by taking the intersection of intersecting ARGs-related genes and intersecting DEGs. The gene ontology (GO) and kyoto encyclopedia of genes and genomes (KEGG) functional enrichment analysis of the intersecting genes was conducted with the "clusterProfiler" package (version 4.4.4) in R [26] (adj. P value < 0.05). Subsequently, the PPI network for intersecting genes was constructed using the STRING database (https://cn.string-db.org/) and candidate genes were obtained (score > 0.4).

Acquisition and validation of biomarkers

First, the expression of the candidate genes was analysed by least absolute shrinkage and selection operator (LASSO) regression using the R package glmnet (version 4.1-8) [27], and the optimal lambda value was determined by 10-fold cross-validation using the cv.glmnet function. Variables with non-zero coefficients at the optimal lambda value were feature genes. Then, the stability of the LASSO model was validated by constructing support vector machine recursive feature elimination (SVM-RFE) and the eXtreme gradient boosting (XGBoost) models. Finally, the diagnostic performance of the characteristic genes was assessed using the pROC package (version 1.18.5) in R [28], and receiver operating characteristic (ROC) with the area under curve (AUC) value > 0.7 were considered as biomarkers in AMI. The expression of biomarkers in AMI and control samples were observed in GSE60993 and GSE61144 and box plots were drawn with the "ggplot2" package (version 3.3.6) in R [29]. In addition, we evaluated the diagnostic performance of these

biomarkers using the "pROC" package (version 1.18.5) [28].

Establishment of alignment diagram and enrichment analysis of biomarkers

Alignment diagram of biomarkers was constructed using the rms package (version 6.3-0) in R [30]. The predictive power of the alignment diagram was assessed using calibration curves. Ingenuity pathway analysis (IPA) of DEGs1 was performed to obtain the relevant pathways, involved in DEGs1, and then the pathways involved in biomarkers were screened. Signalling pathways with $P<0.05$ were selected and ranked according to -log(P); z-score > 2 indicates that the pathway is activated and z-score <-2 indicates inhibition. In addition, the signalling pathway with the largest |z-score| ranking and significance was selected to demonstrate the effect of the biomarker on signalling in that signalling pathway. Finally, Gene set enrichment analysis (GSEA) for biomarkers was conducted based on KEGG genes sets with ClusterProfiler package (version 4.4.4) in the GSE60993 [31] (adj. Pvalue < 0.05, |NES|>1).

Immune analysis, drug prediction and molecular Docking

The immune abundance of 22 immune cells in the AMI and control samples of the GSE60993 was calculated using the CIBERSORT algorithm [32]. Differential immune cells were compared between AMI and control samples using the wilcox test ($P<0.05$), and correlations between biomarkers and differential immune cells were calculated using spearman. The drugs for the biomarkers were predicted using the Drug-Gene Interaction database (DGIdb, https://www.dgidb.org/) and the drugs were visualized using PubChem database (https://pubchem.ncbi.nlm.nih.gov/).

Establishment of regulatory network

Differentially expressed miRNAs (DE-miRNAs) and differentially expressed lncRNAs (DE-lncRNAs) were obtained by differential expression analysis in the GSE24548 and GSE97320 datasets using the limma package (version 3.52.2) by setting $|\log_2 FC| > 0.5$ and $P<0.05$ [25]. In addition, miRNAs for biomarkers were predicted by using the miRWalk database (http://mirwalk.umm.uni-heidelberg.de/), and the intersecting miRNAs were obtained by take intersection of miRNAs and DE-miRNAs. The lncRNAs of the intersecting miRNAs were obtained by starbase database (https://starbase.sysu.edu.cn/starbase2/index.php), and the intersecting lncRNAs were obtained by taking the intersection of lncRNAs and DE-lncRNAs. The relationship pairs of upregulated mRNAs, downregulated miRNAs, and upregulated lncRNAs were generated, meanwhile, the relationship pairs of downregulated mRNAs, upregulated miRNAs, and downregulated lncRNAs were generated as well. Based on this, the lncRNA-miRNA-mRNA network maps were constructed.

Clinical samples collection, RNA extraction and quantitative PCR (qPCR)

From February 27, 2023 to March 13, 2023, we collected 10 ml blood samples from 10 patients with acute myocardial infarction (acute coronary syndrome patients who received direct percutaneous coronary intervention within 4 h after chest pain onset) and 10 healthy individuals who underwent physical examination at Shanxi Norman Bethune Hospital (with normal coronary angiography). Collect blood samples and store them at 2–6 ℃. QPCR is used to detect the expression levels of biomarkers in clinical blood samples. All samples were lysed with TRIzol Reagent, and total RNA was isolated following the manufacturer's instructions. The extracted RNA was reverse-transcribed to cDNA using the SureScript-First-strand-cDNA-synthesis-kit before qPCR. The qPCR reaction consisted of 3 μl of reverse transcription product, 5 μl of 2xUniversal Blue SYBR Green qPCR Master Mix, and 1 μl each of forward and reverse primer. PCR was performed in a BIO-RAD CFX96 Touch TM PCR detection system (Bio-Rad Laboratories, Inc., USA) under the following conditions: initial denaturation at 95℃ for 1 min, followed by 40 cycles that each involved incubation at 95℃ for 20 s, 55℃ for 20 s, and 72℃ for 30 s. The detailed forward and reverse primers were shown in the Supplementary Table 2. All primers were synthesized by Servicebio (Servicebio, Wuhan, China). The GAPDH served as an internal control, and the relative expression of biomarkers was determined using the $2^{-\Delta\Delta Ct}$ method. The experiment was repeated in triplicate on independent occasions. Statistical differences in the five biomarkers between AMI samples and control samples were detected by paired t-test using GraphPad Prism 5.

Statistical analysis

Bioinformatics analysis was proceeded in R software. Wilcoxon test was employed in immune infiltration analysis between AMI and control samples. Statistical differences for biomarkers expressions between clinical AMI samples and control samples were detected by paired t-test.

Results

2,739 intersecting ARGs-related genes were identified by the GSVA and WGCNA

The GSVA in AMI and control samples in the GSE60993 dataset results showed that there were significant differences in scores of ARGs between the AMI and control samples ($P<0.01$, Fig. 1a). A total of 7,349 ARGs-related

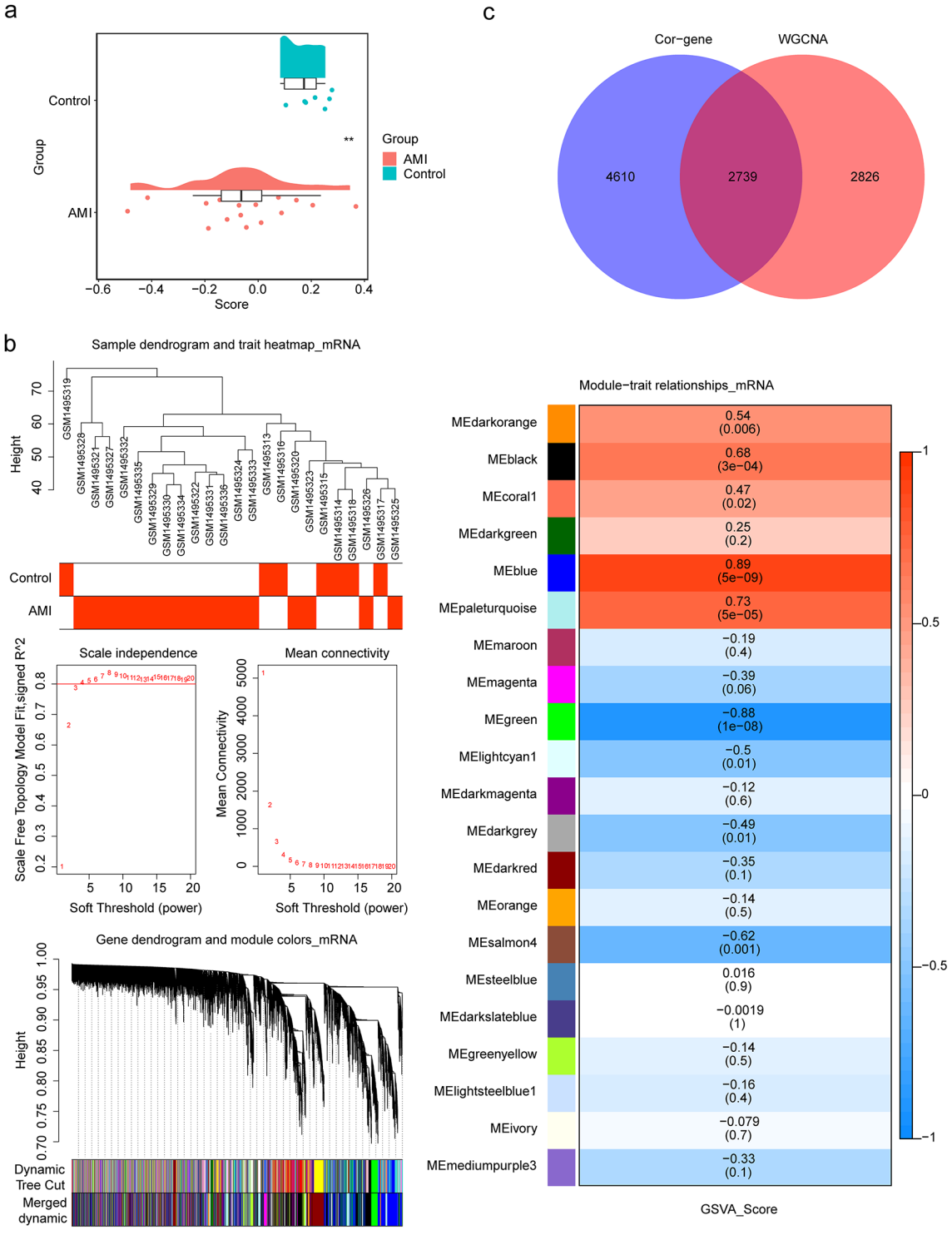

Fig. 1 Identification of histone acetylation regulatory genes (ARGs)-related genes. (**a**) Gene set variation analysis (GSVA) analysis displayed the scores of ARGs of AMI and control samples in the GSE60993 dataset. (**b**) Weighted Gene Co-Expression Network to identify key modules related to scores of ARGs, including sample clustering dendrogram and trait heatmap to remove outliers, Analysis of the scale-free fit index (left) and the mean connectivity (right) for various soft-thresholding powers, cluster dendrogram of all DEGs based on similar expression patterns, and correlations heatmap between modules and traits were showed. (**c**) Venn diagrams for 2,739 ARGs-related genes

genes were obtained (Supplementary Table 3). The soft threshold in the WGCNA analysis was finally set to 4, the adjacency and dissimilarity coefficients between genes were calculated, and the tree was divided into different modules using dynamic cropping methods, and the blue module which contained 5,565 genes was the most relevant module for AMI were obtained (|Cor|> 0.5, $P < 0.05$, Fig. 1b). A total of 2,739 intersecting ARGs-related genes are obtained by overlapping the key module and ARGs-related genes (Fig. 1c).

There were 18 intersecting genes related histone acetylation in AMI

A total of 996 DEGs1 were obtained from GSE60993, of which 576 were up regulated and 417 down regulated (Fig. 2a, b). A total of 66 DEGs2 were obtained from GSE48060, of which 23 were up-regulated and 43 down-regulated (Fig. 2c, d). A total of 25 intersecting DEGs were obtained by taking the intersection of DEGs1 and DEGs2 (Fig. 2e). A total of 18 intersecting genes were obtained by taking the intersection of 2,739 intersecting ARGs-related genes and 25 intersecting DEGs (Fig. 2f). The GO entries enriched by intersecting genes such as cell killing, animal organ regeneration, and defense response to bacterium (Fig. 2g). The KEGG entries were enriched by intersecting genes such as graft-versus-host disease, viral myocarditis, and natural killer cell mediated cytotoxicity (Fig. 2h). To explore whether interactions existed between the 18 intersecting genes, a PPI network was created (Fig. 2i) and obtained 11 candidate genes, among which there are strong interactions between ANXA3 and S100A12, GZMB and PRF1.

Five biomarkers were determined by machine learning, ROC, and qPCR

When lambda.min was 0.082 the results of LASSO regression analysis were selected to obtain five characteristic genes, which were AQP9, HLA-DQA1, MCEMP1, NKG7, and S100A12 (Fig. 3a). The stability of the LASSO model was validated by SVM-REF and XGboost models (AUC > 0.9) (Fig. 3b, Supplementary Fig. 2). The ROC curves of the characteristic genes in the GSE60993 and GSE48060 datasets were plotted in Fig. 3c, and the result shows that the control and AMI samples in the GSE60993 and GSE48060 datasets were well distinguished by all five characteristic genes (AUC > 0.7). In addition, the expression trends of five biomarkers were consistent in the training and validation sets (Fig. 3d). The qPCR was used to verify the expression levels of biomarkers and the results showed that the expression of other biomarkers was consistent with training and validation sets, except for NKG7 (Fig. 3e).

The biomarkers were enriched in ribosomes by IPA and GSEA analyses

Alignment diagram of five biomarkers was constructed (Fig. 4a). The calibration curves and decision curves show that the alignment diagram has good predictive performance (Fig. 4b). The results of IPA analysis show that biomarkers are involved in two pathways including MSP-RON signalling in macrophages pathway and PD-L1 cancer immunotherapy pathway which were activated, and five pathways including COS-ICOSL signalling in T helper cells and calcium-induced T lymphocyte apoptosis which were inhibited (Fig. 4c). In addition, the effect of biomarkers on signalling in the |z-score| top-ranked signalling pathway (calcium-induced T lymphocyte apoptosis) is shown in Fig. 4d. In order to understand how biomarkers may be involved and influence the onset of AMI, GSEA was performed. The KEGG entries involved in biomarkers including ribosome, DNA replication, and allograft rejection (Fig. 4e).

Four immune cells and 14 drugs were identified as associated with the biomarkers

To explore whether the biomarkers could influence AMI patient prognosis by affecting immunity, an immune analysis was completed. Four immune cells (neutrophils, resting NK cells, resting CD4 memory T cells, CD8 T cells) were differentially expressed in AMI and control samples ($P < 0.5$, Supplementary Fig. 3.). Correlations between these four differential immune cells and biomarkers were calculated, and there was a strong correlation between all of the differential immune cells and biomarkers expression (|cor|>0.3 and $P < 0.5$, Fig. 5a). To explore which drugs the biomarkers might be affected by, drug predictions were completed in the DGIdb database and a total of 14 drugs were obtained, as shown in Supplementary Table 4. The structure of the highest scoring drug atogepant was visualized. We selected ATOGEPANT for molecular docking with S100A12, which has a binding energy of – 10 kcal/mol (Fig. 5b).

A lncRNA-miRNA-mRNA regulatory network was constructed

A total of 79 DE-miRNAs and 353 DE-lncRNAs were obtained from GSE24548 and GSE97320, separately (Supplementary Fig. 4a-d). And meanwhile, 774 miRNAs for biomarkers were predicted, and four intersecting miRNAs (hsa-miR-199a-5p, hsa-miR-139-3p, hsa-miR-140-5p, and hsa-miR-548d-5p) were obtained by take intersection of 774 miRNAs and 79 DE-miRNAs (Supplementary Fig. 4e). 175 lncRNAs for four intersecting miRNAs were predicted, and 12 intersecting lncRNAs (MALAT1, FTX, PRKCQ-AS1, LINC00886, NEAT1, LINC00667, LINC00313, LINC01133, LINC00944, LINC00691, LINC00662, SNHG9) were obtained by

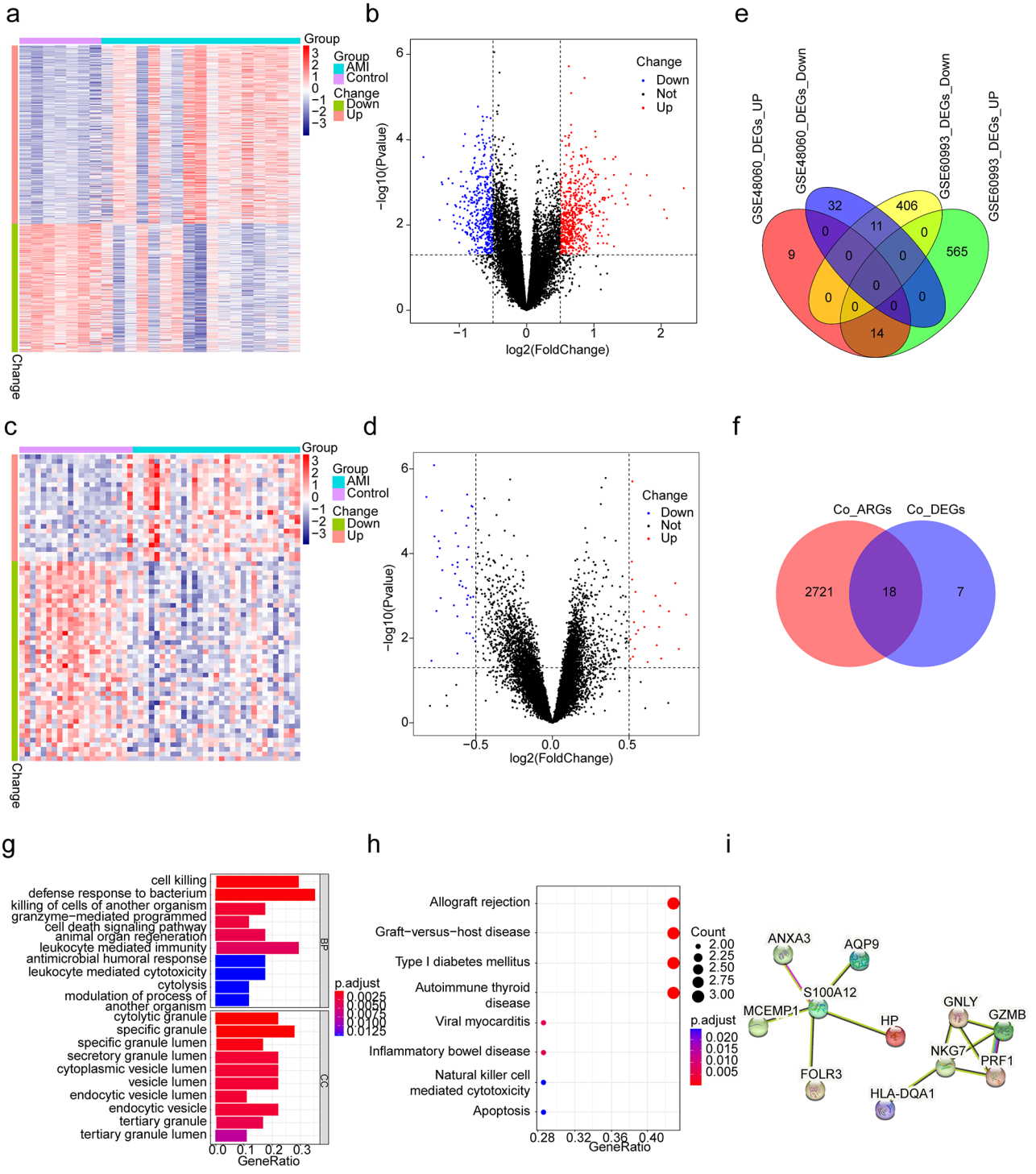

Fig. 2 Collection and functional enrichment analysis of key intersecting genes. (**a**) Heatmap and (**b**) Volcano plot of 996 differentially expressed genes (DEGs) between the AMI and control samples in GSE60993. (**c**) Heatmap and (**d**) Volcano plot of 66 DEGs between the AMI and control samples in GSE48060. The screening criteria are set to $|Log_2FC| > 0.5$ and $P < 0.05$. (**e**) Venn diagrams for 25 intersecting DEGs in two AMI-related cohorts. (**f**) Venn diagrams for 18 intersecting ARGs-related DEGs in AMI. (**g**) The Gene Ontology (GO) analysis for intersecting ARGs-related DEGs. (**h**) The most enriched Kyoto Encyclopedia of Genes and Genomes (KEGG) terms of intersecting ARGs-related DEGs. (**i**) The protein-protein interaction (PPI) network for intersecting ARGs-related DEGs

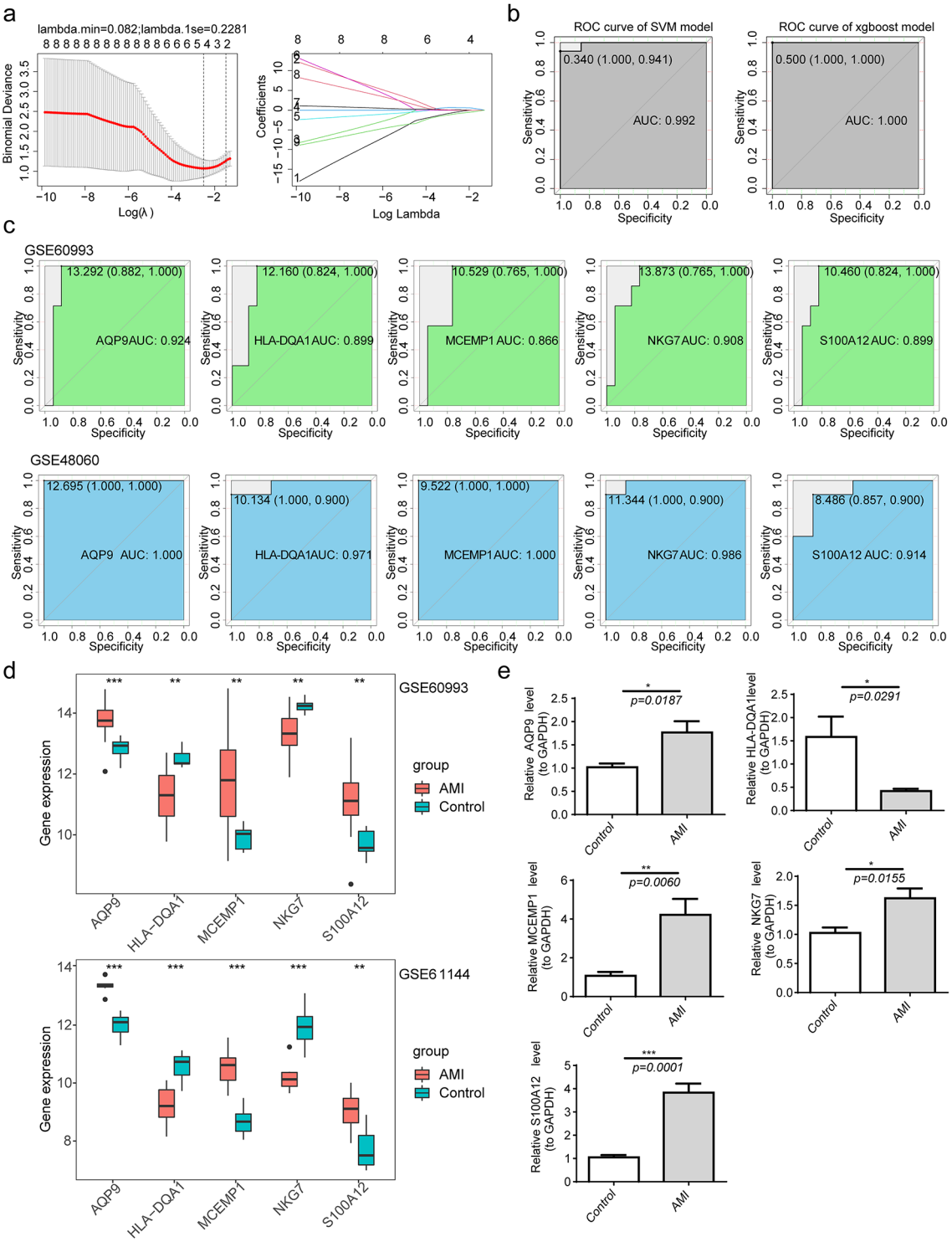

Fig. 3 Screening of five biomarkers in AMI. (**a**) Cross-validation for tuning parameter selection in the least absolute shrinkage and selection operator (LASSO) Cox model was shown and five characteristic genes were selected. (**b**) Receiver operating characteristic (ROC) curves of the LASSO model-based genes in the support vector machine recursive feature elimination (SVM-RFE) and the extreme gradient boosting (XGBoost) algorithms. (**c**) ROC analysis of five characteristic genes in the GSE60993 and GSE48060 datasets. (**d**) Boxplots for the expression levels of five characteristic genes in the GSE60993 and GSE48060 datasets. (**e**) Results of quantitative PCR (qPCR) for the expression levels of five characteristic genes in the clinical AMI and normal blood samples. * $P < 0.05$, ** $P < 0.01$, *** $P < 0.001$

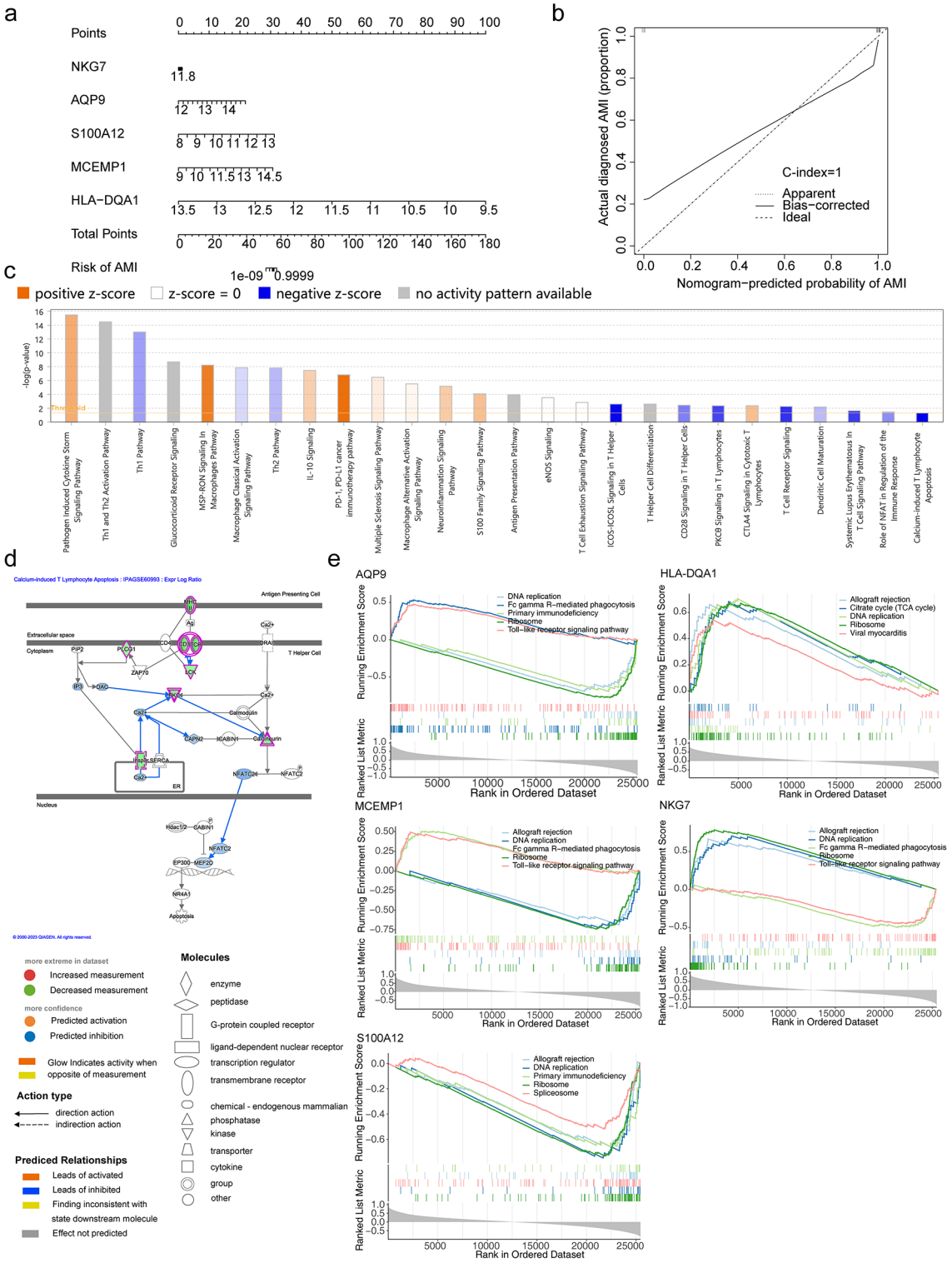

Fig. 4 Construction of the nomogram and analysis of five biomarkers. (**a**) Nomogram was constructed based on five biomarkers. (**b**) Calibration curve of nomogram (C-index = 1). **c-d**) Bar chart of enriched canonical pathways of DEGs between the AMI and control samples in GSE60993 was exhibited using the Ingenuity Pathway Analysis (IPA), where orange represents activation, blue represents inhibition, in which the effect of biomarkers for the signalling pathway of calcium-induced T lymphocyte apoptosis was further mapped. **e**) Gene set enrichment analysis (GSEA) results of five biomarkers

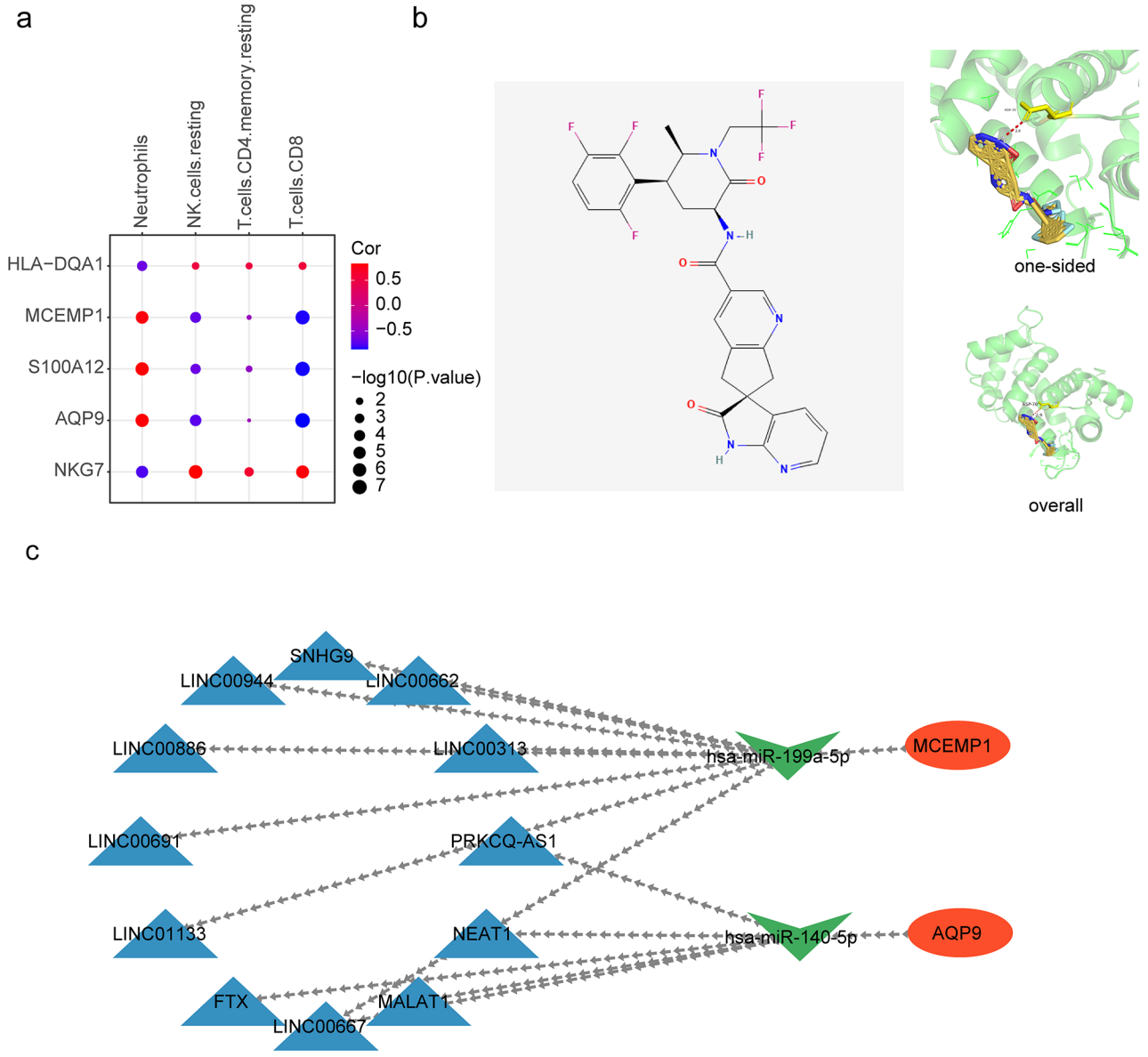

Fig. 5 Immune related analyses and drug prediction targeted biomarkers. (**a**) Pearson correlation heatmap between five biomarkers and four differential expressed immune cells. (**b**) The structure of the highest scoring drug ATOGEPANT, and molecular docking results of targets and ATOGEPANT using AutoDock. (**c**) The lncRNA-miRNA-mRNA regulatory network diagram. Blue represents lncRNAs, green represents miRNAs, and red represent biomarkers

take intersection of 175 lncRNAs and 353 DE-lncRNAs (Supplementary Fig. 4f). The lncRNA-miRNA-mRNA networks was constructed with 16 edges and 15 nodes (Fig. 5c), both mRNAs and lncRNAs are upregulated and miRNAs are downregulated in this network such as MCEMP1 upregulate, hsa-miR-199a-5p downregulate, LINC00313 upregulate and other relationship pairs.

Discussion

Considering the great harm of AMI and the rapid change of many patients' conditions, clinical attention is paid to the early clinical diagnosis of suspected patients, so as to confirm the diagnosis and implement targeted treatment for patients as soon as possible. However, some patients still cannot get a timely, effective, and accurate diagnosis, which affects the prognostic effect of clinical treatment [33, 34]. In the past, many scholars have conducted in vitro myocardial cell hypoxia/reoxygenation (H/R) and in vivo I/R experiments, and through analysis of a large number of experimental results, studies have found that many epigenetic factors are involved in the pathogenesis of AMI, and have different effects [35, 36]. Meanwhile, previous studies have also shown a close relationship between changes in epigenetic expression and an increase in myocardial infarction area and cardiac dysfunction during myocardial I/R [37]. This study used 77

histone acetylation regulatory genes (ARGs) as the background gene set for gene set variation analysis (GSVA), and ultimately identified a new set of biomarkers (AQP9, HLA-DQA1, MCEMP1, NKG7, S100A12) whose functions and pathways may directly or indirectly affect the occurrence and development of acute myocardial infarction. In addition, the column chart constructed based on biomarkers has good predictive performance. Based on the conclusions drawn from this study, it is found that in the process of clinical analysis, diagnosis, and treatment planning for patients with acute myocardial infarction, relevant biomarkers and targets can be actively identified from the field of epigenetics [8].

Analysis of GSEA results reveals that enrichment pathways are related to inflammatory and immune response pathways. The occurrence of AMI is mainly related to atherosclerosis, so this disease is also regarded as a disease caused by chronic inflammation [38]. Some signalling pathways in macrophages and tumour necrosis factor signalling pathways are involved in related inflammatory responses and may have some adverse effects on patients with AMI [39]. These pathways are closely related to AMI. In atherosclerotic plaque, a large number of chemotactic circulating immune cells will participate in the process of endothelial damage and lipid infiltration [40]. And Neutrophils are a very important cell type in the progression of atherosclerosis, and play a significant role in promoting disease progression. Neutrophils can release a large number of different types of adhesion factors and cytokines, promote the increase of plaque area, and enhance its stability [41], In addition, neutrophils also have a positive promoting effect on macrophage phagocytosis of lipids and promote the elevation of MMP-9 levels [42, 43]. Notably, there was a strong association between immune-related genes and AMI, and this was also the case with immune cells, as reported in another independent study [44]. In this study, the obtained research results reiterated the close correlation between these pathways and CAD, indicating that we should continue to pay attention to related issues. Through the observation and analysis of the results obtained by some scholars in the past, it can be found that there is a certain relationship between the occurrence of cardiovascular diseases and HLA-DRB1 and DQA1 genomes [45]. There are some potential biomarkers for AMI, and these biomarkers can provide new targets for clinical treatment of patients with this kind of disease. Studies have found that overexpression of S100A12 may cause excessive inflammatory response, and at the same time, it also leads to certain oxidative stress responses, which are related to AMI to a certain extent [37]. Therefore, this indicator can be used as a potential biomarker for AMI. Meanwhile, the results also demonstrate that the five characteristic biomarkers play a crucial role in AMI. In addition, after analysing the results of certain studies, it is not difficult to find that there are certain correlations between biomarkers and differentially expressed immune cells, such as NK cells resting was negatively correlated with AQP9.

In the acute stage of cardiac injury, blood flow will suddenly stop, leading to the occurrence of myocardial infarction and various inflammatory reactions. In addition, once the dead cells begin to die, the priming of the innate immune system is triggered, and this priming process occurs immediately, accompanied by the onset of myocardial infarction [43]. There is a certain correlation between neutrophils and the occurrence of infarct tissue injury [46], the effect is reflected in many aspects, such as promoting the reduction of inflammatory levels, positively promoting wound healing, etc [43]. Therefore, in the process of treating AMI patients, bioinformatics analysis can be actively carried out to identify markers related to the degree of immune cell infiltration, in order to better guide the development of clinical treatment plans. Previous animal experiments have shown a certain correlation between the high expression of the immune-related gene AQP9 and immune cells in AMI mouse models. AQP9 has the strongest positive correlation with neutrophils and the strongest negative correlation with T cell CD8 [47], which proves that the results of this study are accurate. A comprehensive analysis of the extensive evidence mentioned earlier, as well as the relevant findings of this study, it is suggested that we should pay attention to and analyse various infiltrating immune cells in the future analysis and research of AMI In vitro, atofen can inhibit CGRP dependent vasodilation in human coronary arteries [48]. Previous studies have found that there are no signals associated with the occurrence of cardiovascular events related to atogipan [49, 50]. During ischemia, CGRP can be used as a rescue molecule. Blocking the CGRP receptor after an ischemic event may worsen the results, as observed in previous studies in mice [51]. Ishii [42] et al. pointed out for the first time through research that there is a correlation between lncRNA MIAT and MI. thirty-four. In addition, some scholars pointed out through the study of peripheral blood related conditions of patients with AMI that abnormal changes in the expression level of MIAT can be observed in peripheral blood cells of patients after AMI, and there is a certain relationship between it and the prognosis of patients [43].

This study constructed an lncRNA miRNA mRNA relationship, in which hsa-miR-199a-5p and hsa-miR-140-5p were downregulated, while SNHG9 was upregulated. Studies have shown that hsa-miR-199a-5p inhibits the migration and invasion of HCC cells by targeting the MAP4K3 promoter, thereby exerting its protective effect [52]. In cardiomyocytes, hsa-miR-199a-5p can protect cardiomyocytes from damage under hypoxic

conditions by targeting HIF1α [53]. On the other hand, hsa-miR-140-5p may inhibit drug induced myocardial cell hypertrophy and other pathological processes at the myocardial level through the mitogen activated protein kinase (MAPK) pathway, particularly the extracellular signal regulated kinase (ERK) pathway. It is worth noting that the elevation of hsa-miR-140-5p in early plasma of patients with acute coronary syndrome (ACS) is mainly derived from coronary endothelial cells (CECs) and monocytes [54]. In addition, studies have found that upregulated SNHG9 is negatively correlated with cardiac function and can mediate the pathogenesis of dilated cardiomyopathy through the miR-326/EPHB3 axis. It is an important regulatory factor in the development of dilated cardiomyopathy [55]. These research results further support the potential roles of hsa-miR-140-5p, hsa-miR-199a-5p, and SNHG9 in cardiovascular disease.

AQP9, HLA-DQA1, MCEMP1, NKG7, S100A12 can serve as a diagnostic biomarker for AMI, NK. cells. resting, all of these cytokines may be involved in the occurrence and development of AMI. In the immunotherapy of AMI patients, the above immune cells may be regarded as important therapeutic targets. However, there are still some limitations to this study. Firstly, the samples are sourced from public databases, and some samples were collected at unspecified times, which may affect the accuracy and clinical application value of biomarkers. In addition, the diversity of sample size and sources may also lead to biased results. Finally, due to the small sample size, it may affect the reliability and generalization ability of the research results. Therefore, in future research, we will strive to expand the sample size to enhance the statistical power of the results; At the same time, strengthen cooperation with clinical institutions to ensure timely and standardized collection of samples, in order to optimize the detection effectiveness of biomarkers. In addition, we will also consider incorporating more key factors that may affect the disease progression to further enhance the depth and comprehensiveness of our research. At the technical level, we will actively explore and apply more advanced detection methods, aiming to improve the detection speed and accuracy of biomarkers, thereby providing more reliable scientific basis for clinical decision-making.

Conclusions

In the study, we identified 18 intersecting genes related to histone acetylation in AMI. Followed by combining LASSO, SVM-RFE, and XGBoost algorithms, the five characteristic genes were obtained, and they were determined as biomarkers by ROC and qPCR verification. These five biomarkers including *AQP9*, *HLA-DQA1*, *MCEMP1*, *NKG7*, and *S100A12* had the potential to diagnose AMI disease from the population. By IPA and GSEA analyses, we found that these biomarkers related to the ribosome, DNA replication, allograft rejection, etc. Interestingly, the neutrophils, resting NK cells, resting CD4 memory T cells, and CD8 T cells were all linked with these biomarkers. In addition, ATOGEPANT related to *S100A12* was predicted, and it could be a potential therapeutic drug in AMI. Together, the five biomarkers identified in this study may provide new insights into the diagnosis of AMI.

Abbreviations

AMI	Acute myocardial infarction
ARGs	Histone acetylation regulatory genes
GEO	Gene expression omnibus
GSVA	Gene set variation analysis
WGCNA	Weighted gene co-expression network analysis
DEGs	Differentially expressed genes
ROC	Receiver operating characteristic
qPCR	Quantitative PCR
CVD	Cardiovascular disease
I/R	Ischemia/reperfusion
PPI	Protein-protein interaction
GO	Gene ontology
KEGG	Kyoto encyclopedia of genes and genomes
LASSO	Least absolute shrinkage and selection operator
SVM-RFE	Support vector machine recursive feature elimination
XGBoost	Extreme gradient boosting
AUC	Area under curve
IPA	Ingenuity pathway analysis
GSEA	Gene set enrichment analysis
DGIdb	Drug-gene interaction database
DE-miRNAs	Differentially expressed miRNAs
DE-lncRNAs	Differentially expressed lncRNAs
H/R	Hypoxia/reoxygenation

Supplementary Information

The online version contains supplementary material available at https://doi.org/10.1186/s12920-025-02135-2.

Supplementary Material 1

Author contributions

Man Li: Conceptualization, Data curation, Investigation, Resources, Software, Visualization, Writing - original draft and Writing - review & editing. Lifeng Yang: Data curation, Investigation, Validation, Visualization, and Writing - review & editing. Yan Wang: Data curation, Investigation, Methodology, Visualization Resources, Software. Lei Zhang: Conceptualization, Data curation, Investigation, Supervision, and Writing - review & editing. All authors read and approved the final manuscript.

Funding

This study was supported by the Shanxi Scholarship Council of China, Research Project [No:2020 – 175]; Shanxi Bethune Hospital (The third Hospital of Shanxi Medical University), Youth Fund [No:2019YJ04].

Data availability

Data availability statement: Five datasets of AMI including GSE60993, GSE48060, GSE61144, GSE24548, and GSE97320 were sourced from the GEO database (https://www.ncbi.nlm.nih.gov/geo/).

Declarations

Ethics approval and consent to participate

This study complies with the Helsinki Declaration. All participants signed informed consent forms, and this study has been approved by the Ethics Committee of Shanxi Norman Bethune Hospital [YXLL-2023-095].

Consent for publication
Not applicable.

Competing interests
The authors declare no competing interests.

Received: 27 February 2024 / Accepted: 27 March 2025
Published online: 18 April 2025

References

1. Liu K, Chen S, Lu R, et al. Identification of important genes related to ferroptosis and hypoxia in acute myocardial infarction based on WGCNA. Bioengineered. 2021;12:7950–63. https://doi.org/10.1080/21655979.2021.1984004
2. Rogers WJ, Frederick PD, Stoehr E, et al. Trends in presenting characteristics and hospital mortality among patients with ST elevation and non-ST elevation myocardial infarction in the National registry of myocardial infarction from 1990 to 2006. Am Heart J. 2008;156:1026–34. https://doi.org/10.1016/j.ahj.2008.07.030
3. Benincasa G, Suades R, Padró T, Badimon L, Napoli C. Bioinformatic platforms for clinical stratification of natural history of atherosclerotic cardiovascular diseases. Eur Heart J Cardiovasc Pharmacotherapy. 2023;9(8):758–69. https://doi.org/10.1093/ehjcvp/pvad059
4. Feng X, Zhang Y, Du M, et al. Identification of diagnostic biomarkers and therapeutic targets in peripheral immune landscape from coronary artery disease. J Translational Med. 2022;20:399. https://doi.org/10.1186/s12967-022-03614-1
5. Aziz M, Jandeleit-Dahm KA, Khan AW. Interplay between epigenetic mechanisms and transcription factors in atherosclerosis. Atherosclerosis. 2024;395:117615. https://doi.org/10.1016/j.atherosclerosis.2024.117615
6. Schiano C, Benincasa G, Infante T, Franzese M, Castaldo R, Fiorito C, Mansueto G, Grimaldi V, Della Valle G, Fatone G, Soricelli A, Nicoletti GF, Ruocco A, Mauro C, Salvatore M, Napoli C. Integrated analysis of DNA methylation profile of HLA-G gene and imaging in coronary heart disease: pilot study. PLoS ONE. 2020;15(8):e0236951. https://doi.org/10.1371/journal.pone.0236951
7. Kim JY, Choi BG, Jelinek J, Kim DH, Lee SH, Cho K, Rha SH, Lee YH, Jin HS, Choi DK, Kim GE, Kwon SU, Hwang J, Cha JK, Lee S, Issa JJ, Kim J. Promoter methylation changes in ALOX12 and AIRE1: novel epigenetic markers for atherosclerosis. Clin Epigenetics. 2020;12(1):66. https://doi.org/10.1186/s13148-020-00846-0
8. Wang K, Li Y, Qiang T, et al. Role of epigenetic regulation in myocardial ischemia/reperfusion injury. Pharmacol Res. 2021;170:105743. https://doi.org/10.1016/j.phrs.2021.105743
9. Herr DJ, Baarine M, Aune SE, et al. HDAC1 localizes to the mitochondria of cardiac myocytes and contributes to early cardiac reperfusion injury. J Mol Cell Cardiol. 2018;114:309–19. https://doi.org/10.1016/j.yjmcc.2017.12.004
10. Xie M, Hill JA. HDAC-dependent ventricular remodeling, trends in cardiovascular medicine, 2013;23:229–35. https://doi.org/10.1016/j.tcm.2012.12.006
11. Qu S, Yang X, Li X, Wang J, Gao Y, Shang R, Sun W, Dou K, Li H, Circular RNA. A new star of noncoding RNAs. Cancer Lett. 2015;365:141–8. https://doi.org/10.1016/j.canlet.2015.06.003
12. Chen KC, Liao YC, Hsieh IC, et al. OxLDL causes both epigenetic modification and signalling regulation on the microRNA-29b gene: novel mechanisms for cardiovascular diseases. J Mol Cell Cardiol. 2012;52:587–95. https://doi.org/10.1016/j.yjmcc.2011.12.005
13. Dje P, N'Guessan, Riediger F, Vardarova K, et al. Statins control oxidized LDL-mediated histone modifications and gene expression in cultured human endothelial cells. Arterioscler Thromb Vasc Biol. 2009;29:380–6. https://doi.org/10.1161/atvbaha.108.178319
14. Jongstra-Bilen J, Zhang CX, Wisnicki T et al. Oxidized Low-Density Lipoprotein Loading of Macrophages Downregulates TLR-Induced Proinflammatory Responses in a Gene-Specific and Temporal Manner through Transcriptional Control, Journal of immunology (Baltimore, Md.: 1950), 2017;199:2149–2157. https://doi.org/10.4049/jimmunol.1601363
15. Greißel A, Culmes M, Burgkart R, et al. Histone acetylation and methylation significantly change with severity of atherosclerosis in human carotid plaques. Cardiovasc Pathology: Official J Soc Cardiovasc Pathol. 2016;25:79–86. https://doi.org/10.1016/j.carpath.2015.11.001
16. Vlad ML, Manea SA, Lazar AG, et al. Histone Acetyltransferase-Dependent pathways mediate upregulation of NADPH oxidase 5 in human macrophages under inflammatory conditions: A potential mechanism of reactive oxygen species overproduction in atherosclerosis. Oxidative Med Cell Longev. 2019;2019(3201062). https://doi.org/10.1155/2019/3201062
17. Ye S, Gale CR, Martyn CN. Variation in the matrix metalloproteinase-1 gene and risk of coronary heart disease. Eur Heart J. 2003;24:1668–71. https://doi.org/10.1016/s0195-668x(03)00385-3
18. Galis ZS, Sukhova GK, Lark MW, et al. Increased expression of matrix metalloproteinases and matrix degrading activity in vulnerable regions of human atherosclerotic plaques. J Clin Investig. 1994;94:2493–503. https://doi.org/10.1172/jci117619
19. Eggers KM. B. Lindahl 2017 Application of cardiac troponin in cardiovascular diseases other than acute coronary syndrome. Clin Chem 2017;63:223–35 https://doi.org/10.1373/clinchem.2016.261495
20. Benincasa G, Marfella R, Della Mura N, Schiano C, Napoli C. Strengths and opportunities of network medicine in cardiovascular diseases. Circulation Journal: Official J Japanese Circulation Soc. 2020;84(2):144–52. https://doi.org/10.1253/circj.CJ-19-0879
21. Lee LY, Pandey AK, Maron BA, Loscalzo J. Network medicine in cardiovascular research. Cardiovascular Res. 2021;117(10):2186–202. https://doi.org/10.1093/cvr/cvaa321
22. Fang Y, Zhao J, Guo X, et al. Establishment, immunological analysis, and drug prediction of a prognostic signature of ovarian cancer related to histone acetylation. Front Pharmacol. 2022;13:947252. https://doi.org/10.3389/fphar.2022.947252
23. Hänzelmann S, Castelo R, Guinney J. BMC Bioinformatics. 2013;14:7. https://doi.org/10.1186/1471-2105-14-7. GSVA: gene set variation analysis for microarray and RNA-seq data.
24. Langfelder P, Horvath S. WGCNA: an R package for weighted correlation network analysis. BMC Bioinformatics. 2008;9:559. https://doi.org/10.1186/1471-2105-9-559
25. Ritchie ME, Phipson B, Wu D, et al. Limma powers differential expression analyses for RNA-sequencing and microarray studies. Nucleic Acids Res. 2015;43:e47. https://doi.org/10.1093/nar/gkv007
26. Sachs MC. PlotROC: A tool for plotting ROC curves. J Stat Softw. 2017;79. https://doi.org/10.18637/jss.v079.c02
27. Friedman JH, Hastie T, Tibshirani R. Regularization paths for generalized linear models via coordinate descent. J Stat Softw. 2010;33(1):1–22. https://doi.org/10.18637/jss.v033.i01
28. Robin X, Turck N, Hainard A, et al. pROC: an open-source package for R and S+to analyze and compare ROC curves. BMC Bioinformatics. 2011;12:77. https://doi.org/10.1186/1471-2105-12-77
29. Wickham H. ggplot2, Wiley Interdisciplinary Reviews: Computational Statistics, 2011;3:180–185.
30. Harrell FE, Harrell F. Harrell, Rms: regression modeling strategies. R Package Version. 2013;4:0–0.
31. Yu G, Wang LG, Han Y, et al. ClusterProfiler: an R package for comparing biological themes among gene clusters. OMICS. 2012;16:284–7. https://doi.org/10.1089/omi.2011.0118
32. Chen B, Khodadoust MS, Liu CL, et al. Profiling tumor infiltrating immune cells with CIBERSORT. Methods Mol Biology (Clifton N J). 2018;1711:243–59. https://doi.org/10.1007/978-1-4939-7493-1_12
33. Wang Q, Liu B, Wang Y, Bai B, Yu T, Chu XM. The biomarkers of key MiRNAs and target genes associated with acute myocardial infarction. PeerJ. 2020;8:e9129. https://doi.org/10.7717/peerj.9129
34. Guihong R, Xiao W, Xinling Q, Yanxia W, Meilian Q, Chunfeng X. Plasma biomarkers for predicting heart failure in patients with acute myocardial infarction. J Med Biochem. 2025;44(1):69–76. https://doi.org/10.5937/jomb0-50741
35. Zhou K, Xu Y, Wang Q, Dong L. Overexpression of miR-431 attenuates hypoxia/reoxygenation-induced myocardial damage via autophagy-related 3. Acta Biochim Biophys Sin. 2021;53(2):140–8. https://doi.org/10.1093/abbs/gmaa154
36. Liao H, Xiao C, Li W, Chen W, Xiang D. Silencing Hsa_circ_0049271 attenuates hypoxia-reoxygenation (H/R)-induced myocardial cell injury via the miR-17-3p/FZD4 signaling axis. Annals Translational Med. 2023;11(2):99. https://doi.org/10.21037/atm-22-6331
37. Su X, Shen Y, Jin Y, Kim IM, Weintraub NL, Tang Y. Aging-Associated differences in epitranscriptomic m6A regulation in response to acute cardiac ischemia/reperfusion injury in female mice. Front Pharmacol. 2021;12:654316. https://doi.org/10.3389/fphar.2021.654316
38. Sun J, Hartvigsen K, Chou MY, et al. Deficiency of antigen-presenting cell invariant chain reduces atherosclerosis in mice. Circulation. 2010;122:808–20. https://doi.org/10.1161/circulationaha.109.891887

39. Xiao J, Moon M, Yan L, et al. Cellular FLICE-inhibitory protein protects against cardiac remodelling after myocardial infarction. Basic Res Cardiol. 2012;107:239. https://doi.org/10.1007/s00395-011-0239-z
40. Zhang J, Yang Z, Liang Z, et al. Secreted frizzled-related protein 4 exerts anti-atherosclerotic effects by reducing inflammation and oxidative stress. Eur J Pharmacol. 2022;923:174901. https://doi.org/10.1016/j.ejphar.2022.174901
41. Zhao T, Jiang Q, Li W, et al. Antigen-Presenting cell-Like neutrophils foster T cell response in hyperlipidemic patients and atherosclerotic mice. Front Immunol. 2022;13:851713. https://doi.org/10.3389/fimmu.2022.851713
42. Davì G, Patrono C. Platelet activation and atherothrombosis. N Engl J Med. 2007;357:2482–94. https://doi.org/10.1056/NEJMra071014
43. Weil BR, Neelamegham S. Selectins and immune cells in acute myocardial infarction and Post-infarction ventricular remodeling: pathophysiology and novel treatments. Front Immunol. 2019;10:300. https://doi.org/10.3389/fimmu.2019.00300
44. Liu J, Chen L, Zheng X, Guo C. Identification of immune-related genes in acute myocardial infarction based on integrated bioinformatical methods and experimental verification. PeerJ. 2023;11:e15058. https://doi.org/10.7717/peerj.15058
45. Moniot A, Braux J, Siboni R, et al. Inhibition of recruitment and activation of neutrophils by Pyridazinone-Scaffold-Based compounds. Int J Mol Sci. 2022. https://doi.org/10.3390/ijms23137226. 23.
46. Carbone F, Nencioni A, Mach F, et al. Pathophysiological role of neutrophils in acute myocardial infarction. Thromb Haemost. 2013;110:501–14. https://doi.org/10.1160/th13-03-0211
47. Zhu X, Yin T, Zhang T, et al. Identification of Immune-Related genes in patients with acute myocardial infarction using machine learning methods. J Inflamm Res. 2022;15:3305–21. https://doi.org/10.2147/jir.S360498
48. Rubio-Beltran E, Chan KY, Danser AJ, et al. Characterisation of the calcitonin gene-related peptide receptor antagonists ubrogepant and Atogepant in human isolated coronary, cerebral and middle meningeal arteries. Cephalalgia: Int J Headache. 2020;40:357–66. https://doi.org/10.1177/0333102419884943
49. Goadsby PJ, Dodick DW, Ailani J, et al. Safety, tolerability, and efficacy of orally administered Atogepant for the prevention of episodic migraine in adults: a double-blind, randomised phase 2b/3 trial, the lancet. Neurology. 2020;19:727–37. https://doi.org/10.1016/s1474-4422(20)30234-9
50. Ailani J, Lipton RB, Goadsby PJ, et al. Atogepant for the preventive treatment of migraine. N Engl J Med. 2021;385:695–706. https://doi.org/10.1056/NEJMoa2035908
51. Mulder IA, Li M, de Vries T, et al. Anti-migraine calcitonin Gene-Related peptide receptor antagonists worsen cerebral ischemic outcome in mice. Ann Neurol. 2020;88:771–84. https://doi.org/10.1002/ana.25831
52. Liu L, Lu L, Zheng A, Xie J, Xue Q, Wang F, Wang X, Zhou H, Tong X, Li Y, Zhu X, Wu G. MiR-199a-5p and let-7c cooperatively inhibit migration and invasion by targeting MAP4K3 in hepatocellular carcinoma. Oncotarget. 2017;8(8):13666–77. https://doi.org/10.18632/oncotarget.14623
53. Chen HY, Lu J, Wang ZK, Yang J, Ling X, Zhu P, Zheng SY. Hsa-miR-199a-5p protect cell injury in hypoxia induces myocardial cells via targeting HIF1α. Mol Biotechnol. 2022;64(5):482–92. https://doi.org/10.1007/s12033-021-00423-7
54. Li XD, Yang YJ, Wang LY, Qiao SB, Lu XF, Wu YJ, Xu B, Li HF, Gu DF. Elevated plasma miRNA-122, -140-3p, -720, -2861, and– 3149 during early period of acute coronary syndrome are derived from peripheral blood mononuclear cells. PLoS ONE. 2017;12(9). https://doi.org/10.1371/journal.pone.0184256
55. Zhang F, Shi H, Xue H, Li H, Li C, Han Q. Up-regulated LncRNA SNHG9 mediates the pathogenesis of dilated cardiomyopathy via miR-326/EPHB3 axis. J Thromb Thrombolysis. 2023;55(4):634–48. https://doi.org/10.1007/s11239-023-02798-7

Publisher's note